# Variability of acoustic signals near a Polar front at the Western Barents Sea

Altan Turgut[1], and Jeffrey Schindall[2]

[1]SoundOceanAI, 1110 S. Washington St., Falls Church, VA 22046, USA
[2]Naval Research Laboratory, Acoustics Div., Washington, DC 20375

Altan Turgut, 1110 S. Washington St., Falls Church, VA 22046, USA,
alturgut@yahoo.com

***Abstract:*** *Analysis of mid-frequency (0.7 to 4 kHz) acoustic data from the October 2022 Barents Sea experiment exhibited the effects of the Polar front, tidal currents, and tidal heights on acoustic travel-time fluctuations. Broadband acoustic model predictions revealed that the primary contribution to the travel-time fluctuations were due to the dynamics of a Polar front in the experimental area. Similar travel-time fluctuations were also calculated using HYCOM-predicted sound speed profiles capturing the dynamics of the Polar front. This implied that use of HYCOM would facilitate a prediction capability of acoustic travel-time fluctuations near a Polar front. In addition, up to 15 dB higher acoustic Transmission Loss (TL) was observed during a major storm event. Measured acoustic Scintillation Index (SI) indicated an unexpected decrease of SI values during this storm event. This SI decrease can be explained by scattering and attenuation of surface-interacting high-angle arrivals and propagation of only more stable low-angle arrivals at a 10 km range. This phenomenon is further investigated by simulating additional scattering mechanisms due to bottom roughness and diffuse background internal waves. Further investigation is underway to include an additional attenuation mechanism due to near-surface bubble layer as well as a 3D out-of-plane scattering.*

***Keywords:*** *Polar front, Travel-time fluctuations, Scintillation Index*

## INTRODUCTION

Amplitude and travel-time variability of mid-frequency acoustic signals near a Polar front is of interest given the scarcity of previous mid-frequency acoustic experiments and theoretical work at high latitudes. Previous experimental and theoretical work by Lynch et al.[1] investigated the effect of diffuse internal waves on low frequency (224 Hz) amplitude and travel-time fluctuation near a Polar Front (PF) in the Barents Sea. Experimental difficulties limited their acoustic data to a cross-front path in which a combination of frontal and internal wave/internal tide signals is present. At lower latitudes, similar studies have been reported to investigate the acoustic scattering by internal waves, surface gravity waves, and fish[2,3]. This paper presents results from a unique experiment providing acoustic and oceanographic data near a PF in the Western Barents Sea covering both cross-front and along-front paths. Therefore, it focuses on the direct effects of a Polar front on the mid-frequency acoustic propagation. In addition, it uses the HYbrid Coordinate Ocean Model (HYCOM) in the acoustic propagation modelling to investigate the travel-time and amplitude fluctuation due to the Polar Front dynamics. Additional effects such as sea-surface roughness, bottom roughness, and diffuse background internal waves are also included in the acoustic propagation modeling.

## EXPERIMENT

The experiment took place near a PF south of Svalbard (Norway) during October 7-17, 2022. Nine oceanographic moorings and three acoustic moorings were deployed within a 25 km by 25 km area. Oceanographic measurements included current, hydrographic, and microstructure observations. Acoustic measurements included transmission of Linear Frequency Modulated (LFM) and Continuous Wave (CW) signals, received at a ~10 km range in cross-front and along-front paths. The source mooring uses an ITC 2010 source, covering a frequency band of 0.7-4.2 kHz. Mid-frequency acoustic data were collected for one-week duration on two 32-channel Vertical Line Arrays (VLAs) with a 77.5 m aperture. Figure 1a shows the locations of the acoustic source and two VLAs in the experimental area. Figure 1b shows the sound-speed at 2 m depth calculated from HYCOM temperature and salinity predictions for October 10, 2022.

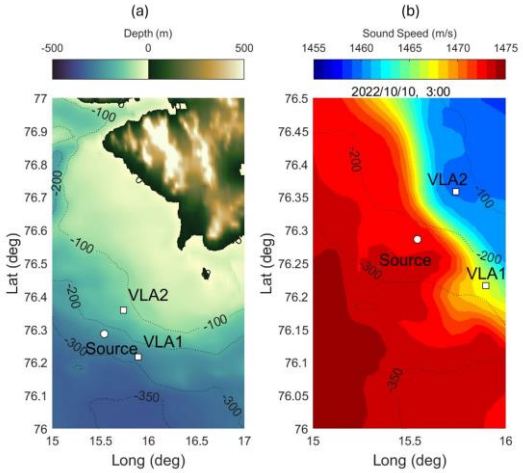


*Fig.1: Experimental area. a) acoustic mooring locations and b) sound-speed at 2 m depth calculated from HYCOM temperature and Salinity data for Oct 10, 2022.*

The colder Arctic water intrusion (low-sound-speed region near Svalbard) in the cross-front path is well predicted by the HYCOM model that is consistent with the Microstructure Vertical Profiler (MVP) measurements. In Figs. 2a and 2b, sound speeds from the MVP measurements and HYCOM predictions are compared along the MVP tracks that was collected during October 11, 2022. In Figs. 2c and 2d, HYCOM predicted sound-speed fields are shown along Source/VLA2 and Source/VLA1 paths, respectively. Figures 2e and 2f show the HYCOM predicted sound-speed fields from Oct 10 to Oct 14, 2022 at 2 m depth along Source/VLA2 and Source/VLA1 paths, respectively. Note in Fig. 2e the intrusion of cold Atlantic water during 10/11/2022 in the Source/VLA2 path with a modulation at M2 tidal period. Time series of temperature and salinity data from the oceanographic moorings also displayed similar variability related to tidal motion with the Arctic and Atlantic waters moving in and out of the Source/VLA2 path.

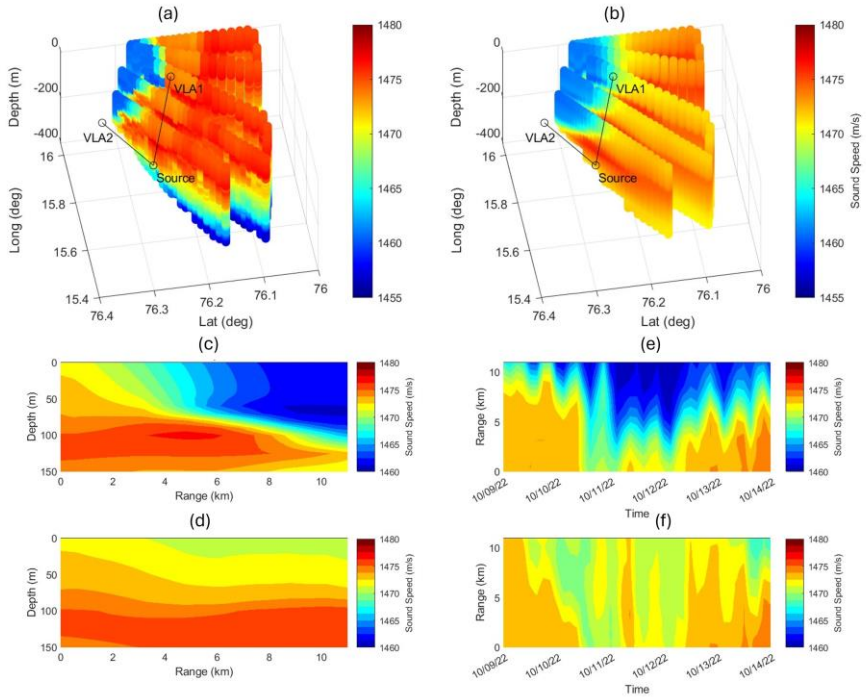


*Fig.2: a) Sound-speed field along the survey track calculated from the MVP measurements, b) sound speed along the survey track predicted from HYCOM, c) sound speed along the source/VLA2 path predicted from HYCOM, d) sound speed along the source/VLA1 path predicted from HYCOM, e) sound speed at 2 m depth along the source/VLA1 path calculated from HYCOM, and f) sound speed at 2 m depth along the source/VLA2 path calculated from HYCOM.*

The ten-day survey was impacted by two major storms with winds around 20 m/s that generated surface waves with significant wave heights above 4 m. Bottom pressure was dominated by semidiurnal fluctuations with a measured tidal-height less than 1.2 m. In this work, starting from Oct 9, 2022 at 18:20UTC, four days of acoustic measurements including the first major storm event are presented. Figure 3 shows 700-1200 Hz, 2-sec long LFM pulses transmitted at every 30 second for four days and received at a VLA1 hydrophone (90 m deep) and at a VLA2 hydrophone (110 m deep). Figs. 3a and 3d show the Matched-Filter (MF) outputs, Figs. 3b and 3e show the peak (MF) outputs, and Figs. 3c and 3f show the relative travel-times for the VLA1 and VLA2, respectively. Note in

Figs. 3a and 3d the stripping of high-angle late arrivals by the first storm event around 50th hour (Oct 12, 2022). In Fig. 1e, peak MF output shows a 15 dB reduction during the storm event at VLA2 hydrophone that is close to the bottom. This was not observed clearly at the VLA1 hydrophone since it was near the mid-water column (see Fig. 3b). Similarly, up to ~50 ms travel-time fluctuations were observed at the VLA2 hydrophone with a M2 tidal period. Travel-time fluctuations and dominance of M2 tidal period were less obvious at the VLA1 hydrophone (see Fig. 3c).

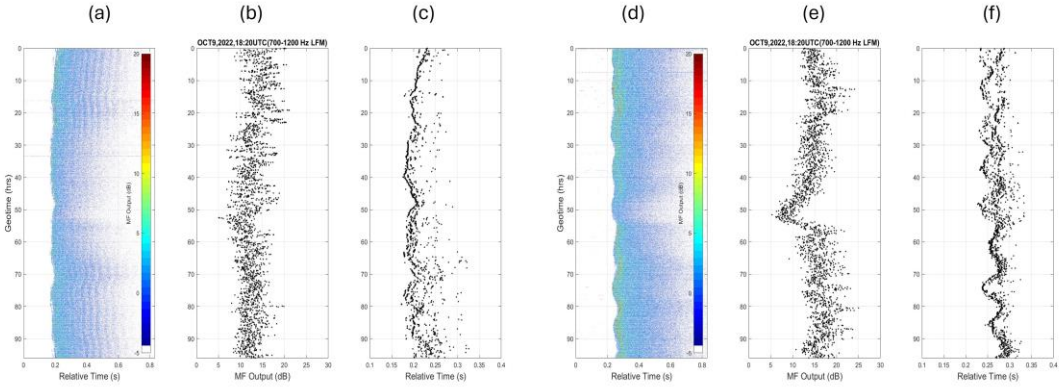


*Fig.3: a,d) Matched-filter outputs of 700-1200 Hz LFM pulses, b,d) peak matched-filter outputs, and c,f) relative travel-time at peak MF outputs at VLA1 and VLA2, respectively*

Figure 4 shows the measured Scintillation Index (SI) of 2-second long 1151 Hz and 2101 Hz CW signals calculated for every 15-minute duration (30 pings with 30-second repetition interval).

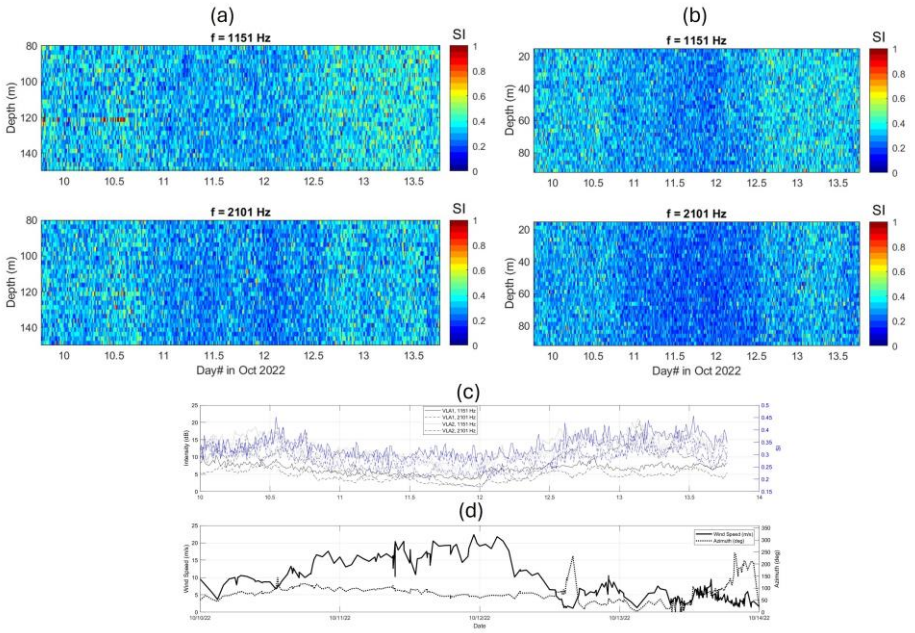


*Fig. 4: a,b) Measured SI of 1151 Hz and 2101 Hz CW signals received at VLA1 and VLA2, respectively, b) depth-averaged acoustic intensity and SI, d) measured wind speed and direction on-board RV HU Sverdrup II.*

The scintillation index values were calculated using the formula

$$SI = \left\langle \left( I - \langle I \rangle \right)^2 \right\rangle / \langle I \rangle^2 , \quad (1)$$

where $I$ is the signal intensity and $\langle I \rangle$ is the average intensity. Note that both measured acoustic intensity and SI are reduced during the major storm event when the wind speed increased to 20 m/s. Decreasing SI at high seas seems to be against the intuition. This will be discussed in the next section with a major numerical simulation effort.

## NUMERICAL SIMULATIONS

To investigate the travel-time and amplitude fluctuations due to the Polar Front dynamics, the HYCOM model outputs are used in the acoustic propagation modelling. The HYCOM ocean model[4] is two-way coupled to the Community Ice CodE (CICE). It has 1/25° (~2.5 km in the study area) horizontal resolution and 41 vertical hybrid coordinate layers. It uses the Navy Coupled Ocean Data Assimilation (NCODA) system for assimilation of satellite surface height anomalies, temperature, and sea ice concentration as well as available in-situ vertical temperature and salinity profiles from XBTs, CTDs, Argo floats, moored buoys and gliders. Observations are assimilated on a 24-hour update cycle. The system is forced with atmospheric momentum and heat fluxes from the 0.17625° 3-hourly Navy Global Environmental Model (NAVGEM). Detailed analysis of oceanographic measurements, modelling, and data processing is available in Jarosz et al.[5] and Schulman at al.[6]

A rough-surface[7] and a 3D[8] Paracolic Equation (PE) model were used to calculate the travel-time and amplitude fluctuations in the area. In Figure 5, a broadband rough-surface PE model was used to investigate the effects of high seas and PF dynamics on broadband (700-850 Hz) acoustic signals. To simulate the sea-surface roughness, JONSWAP spectra were used with different wind speeds and a 100 km fetch. The pulse signal $p(t)$ is obtained by a Fourier synthesis of CW runs within 700 Hz and 850 Hz. Then, transmission loss of the pulse signal defined as $TL(t) = -20\log_{10}\left(\left|p(t)\right|^2\right)$.

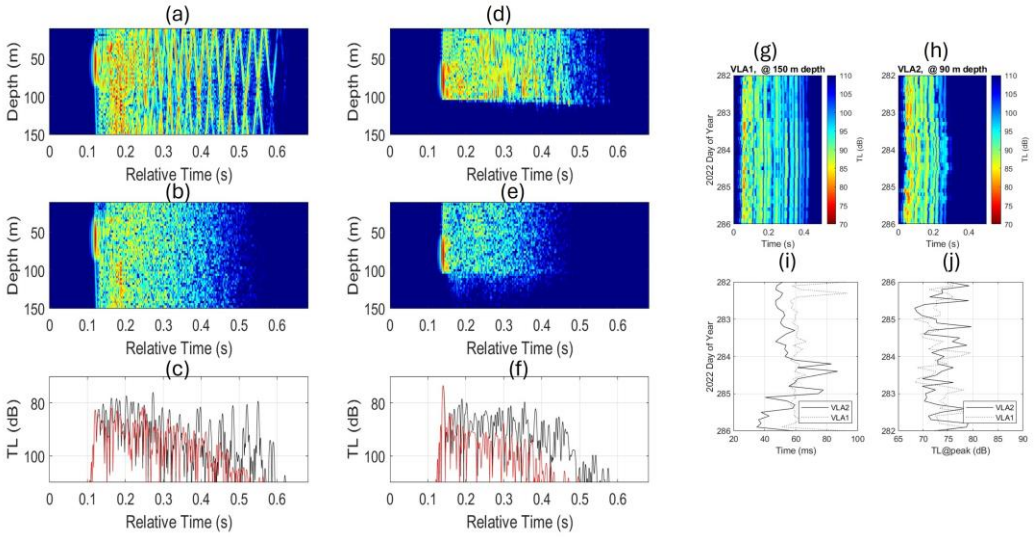

*Fig. 5: a,b,c) comparison of 700-850 Hz signals received at VLA1 for flat surface and rough surface (wind speed: 20 m/s), d,e,f) comparison of 700-850 Hz signals received at VLA2 for flat surface and rough surface (wind speed: 20 m/s), g) modelled travel-time fluctuations at VLA1 using HYCOM predictions, h) modelled travel-time fluctuations at VLA2 using HYCOM predictions, i) relative arrival times at VLA1 and VLA2, and j) modelled TL fluctuations at VLA1 and VLA2.*

In 5a, 5b, and 5c, comparison of broadband signals for the source/VLA1 path are shown for both a flat surface and a rough surface with a wind speed of 20 m/s. In 5d, 5e, and 5f, comparison of broadband signals for the source/VLA2 path are shown for a flat surface and rough surface with a wind speed of 20 m/s. Figures 5g and 5h show the modelled travel-time fluctuations due to the PF dynamics predicted by HYCOM data at every 3 hours (see Figs. 2e and 2f). Note in Fig. 5i that cross-front path has more travel-time fluctuations after the cold Arctic water intrusion starts on Year Day 284 (Oct 12, 2022). The model predicts ~40 ms travel-time fluctuations from HYCOM-predicted PF dynamics that is comparable with those of the measurements. The model also predicts a 3 ms travel-time variation for an 80 cm/s tidal current and a travel-time value of 0.3 ms for a 1.2 m tidal height. Also note in Fig. 5j that, there is ~ 10 dB TL fluctuations on both cross-front and along-front paths.

In Fig.6, probability density functions (pdfs) of measured SIs are compared with modelled SIs for 1151 Hz and 2101 Hz signals. As a reference, median SIs (50 percentile)

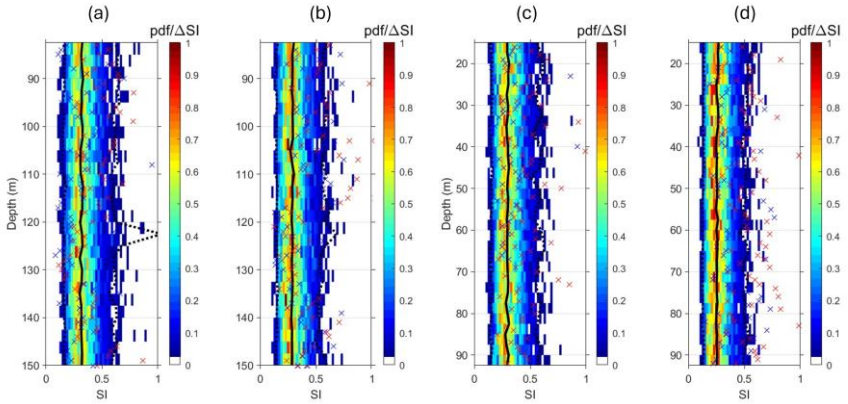


*Fig. 6: a,b) Normalized pdfs of measured SI at VLA1 for 1151 Hz and 2101 Hz, respectively, c,d) normalized pdfs of measured SI at VLA2 for 1151 Hz and 2101 Hz, respectively. Model-predicted SIs are overlayed for a 5 m/s wind (blue x marks) and a 20 m/s wind (red x marks).*

are plotted as black lines. In addition, 2.5 and 97.5 percentiles are plotted as dotted black lines. Median SI values of measured SIs were ~0.35 that did not show a depth dependence and indicated an unsaturated regime at VLA1 (12 km range) and VLA2 (10 km range). The modelled SI values were generated by rough-surface PE using 30 rough see-surface realizations for a 5 m/s wind (blue x marks) and 20 m/s wind (red x marks). The modelled SI values are slightly larger than the measured SIs. In addition, results show slight increase of SI values for the 20 m/s wind. Additional scattering mechanisms including rough-bottom and diffuse internal waves were also added in the rough-surface PE model (not shown in this paper) that did not change the results of SI values being slightly higher at higher winds. Additional attenuation mechanisms for the high angle arrivals (e.g., near-surface bubble layer, 3D scattering) might be needed to verify the measurements.

Increase of TL during the storm event was also studied using a 3D rough-surface PE model to investigate the interaction of surface gravity waves as well as a range/azimuth dependent bottom near a PF. Figure 7 shows the TL at 10 km range for a 700 Hz CW signal. Figures 7a and 7b show the TL predictions for a flat sea-surface using the HYCOM data for Oct 10 and Oct 13, respectively. Figure 7c compares the depth-averaged TL for these two cases. Considering the minor TL differences and relatively minor azimuthal dependence, dynamics of PF did not produce significant horizontal refraction. Figures 7d and 7e show the TL predictions for a rough sea surface generated by a 20 m/s wind coming from NW (45 deg. azimuth) direction during Oct 10 and Oct 13, respectively. Figure 7f compares the depth-averaged TL for these two cases. Difference between predicted TL for Oct 10 and 13 seems to be minor. However, there is a significant azimuthal dependency of TL due to interaction of directional surface gravity waves and range/azimuth dependent bathymetry. Further analysis of measured acoustic data will be conducted to investigate the azimuthal dependency due to surface gravity waves and highly variable bathymetry.

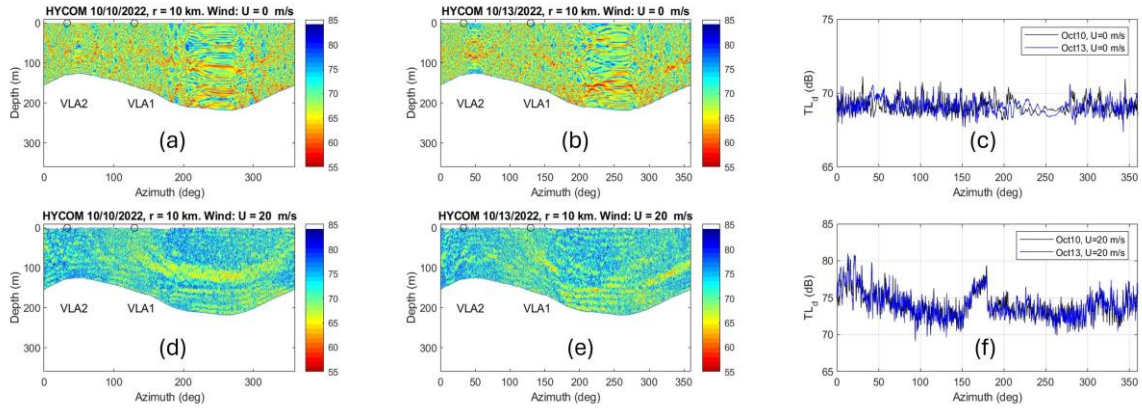


*Fig. 7: a,b) TL predictions for a flat surface using the HYCOM data for Oct 10 and Oct 13, c) depth-averaged TL for a flat surface using the HYCOM data for Oct 10 and Oct 13, d,e) TL predictions for a rough surface using the HYCOM data for Oct 10 and Oct 13, f) depth-averaged TL for a rough surface using the HYCOM data for Oct 10 and Oct 13,*

## SUMMARY

This paper presents extensive field measurement and numerical simulation results to better understand the acoustic travel-time and amplitude fluctuations in the vicinity of a Polar front. Several experimental observations have been made during a four-day acoustic and oceanographic measurements. First, up to 50 ms of travel-time variations were observed especially after the Polar front moved into the Source/VLA2 propagation path. Second, a slight decrease of the Scintillation Index values was observed during a major storm event. Numerical simulations showed that higher sea states produced slightly increased SI values that contradicts with the observations. Inclusion of additional scattering due to bottom roughness and diffuse internal waves did not change the fact that higher sea states produced slightly increased SI values. Inclusion of a near surface bubble layer as an additional attenuation mechanism, and 3D modelling to include additional (out-of-plane) scattering mechanism was left for the future work. Extensive mid-frequency

acoustic propagation modelling and use of 3D HYCOM data provided a realistic model/data comparison as well as a sonar prediction capability. Broadband acoustic model predictions revealed that the primary contribution to the travel-time fluctuations were due to the dynamics of a Polar front in the experimental area. In addition, acoustic modelling with HYCOM data produced amplitude fluctuations comparable to those of measurements. This implied that use of HYCOM would facilitate a prediction capability of acoustic travel-time and amplitude fluctuations near a Polar front.

## ACKNOWLEDGEMENTS

This work was supported by the US Office of Naval Research. We thank the PI Ewa Jarosz for the collection and analysis of oceanographic data. The help from the captain and crew of the RV HU Sverdrup II is greatly appreciated.

## REFERENCES

[1] **J. F. Lynch, G. Jin, R. Pawlowicz, D. Ray, A. J. Plueddemann, C-S Chiu, J. H. Miller, R. H. Bourke, A. R. Parsons, and R. Muenchuthors,** Acoustic travel-time perturbations due to shallow-water internal waves and internal tides in the Barents Sea Polar Front: Theory and experiment, *J. Acoust. Soc. Am. 99 (2), pp. 803-821, 1996.*

[2] **D. E. Weston,** 'Mechanisms of ocean acoustic attenuation: Scattering by internal solitons, by sea surface waves, and by fish, *J. Acoust. Soc. Am. 92, pp. 3435–3437, 1992.*

[3] **D. Rubenstein and M. H. Brill, '***Acoustic variability due to internal waves and surface waves in shallow water, in Ocean Variability and Acoustic Propagation,* Editors: J. Potter and A. Warn-Varnas, Kluwer Academic, *pp. 215–228, Dordrecht, 1991.*

[4] **R. Bleck,** An oceanic general circulation model framed in hybrid isopycnic-Cartesian coordinates. Ocean Model 4: pp 55–88, 2002.

[5] **E. Jarosz, A. Turgut, H. Wikesekera, I. Schulman, and C. Luecke,** Observations on dynamics of the Polar Front south of Svalbard, Norway, *AGU Ocean Sciences Meeting,* HE43A-08, Feb 2024, New Orleans, LA.

[6] **I. Schulman, E. Jarosz, S. Cayula1, and E. J. Metzger,** Dynamics of the Polar Front in the southwestern area of Svalbard, Norway, Ocean Dynamics,74, pp 637–653. 2024.

[7] **M. D. Collins, A. Coury A., and W. L. Siegmann,** Beach acoustics. J. Acoust. Soc. Am., 87 97(5), pp. 2767–2770, 1995.

[8] **M. D. Collins and S. A. Chin-Bing,** A three-dimensional parabolic equation model that includes the effects of rough boundaries, J. Acoust. Soc. Am., 87, pp. 1104–1109. 1990.